Version of Record: https://www.sciencedirect.com/science/article/pii/S1278321820300068
Manuscript_783fee90fa91af6cbcf93d97eb9d54cd

Implementation of an optimization method for parotid gland sparing during inverse planning for head and neck cancer radiotherapy

Implémentation d'une méthode optimisée pour l'épargne des glandes parotides lors de la planification d'arcthérapie volumétrique modulée (VMAT) des cancers ORL

Nolwenn Delaby[a]*, Sandrine Martin[b], Anaïs Barateau[c], Olivier Henry[a], Nicolas Perichon[a], Renaud De Crevoisier[c], Enrique Chajon[b], Joël Castelli[c], Caroline Lafond[c]

[a]*Centre Eugène Marquis, Unité de Physique Médicale, rue de La Bataille Flandres Dunkerque – CS 44229 – 35042 Rennes Cedex, France*
[b]*Centre Eugène Marquis, Département de Radiothérapie, rue de La Bataille Flandres Dunkerque – CS 44229 – 35042 Rennes Cedex, France*
[c]*Univ Rennes, CLCC Eugène Marquis, INSERM, LTSI - UMR 1099, F-35000 Rennes, France*

*Corresponding author: Nolwenn Delaby, Service de Physique Médicale, Centre Eugène Marquis – Rue de La Bataille Flandres Dunkerque – CS 44229 – 35042 Rennes Cedex. Tel: +33 2 99 25 29 75; Fax: +33 2 99 25 30 33; E-mail: n.delaby@rennes.unicancer.fr

Conflit d'intérêt : aucun

Titre courant : Optimization method for parotid gland sparing

© 2020 published by Elsevier. This manuscript is made available under the CC BY NC user license
https://creativecommons.org/licenses/by-nc/4.0/

Résumé

Objectif de l'étude : Afin d'épargner les glandes parotides lors d'une planification dosimétrique de la sphère ORL en arcthérapie volumétrique modulée (VMAT), un modèle basé sur la superposition de volumes cible prévisionnel (PTV) et des organe à risque (Moore et al.) a été développé et évalué.

Matériels et méthodes : les dossiers de 160 patients traités pour un cancer ORL localement évolué ont été considérés. Une optimisation du modèle a été réalisée avant son évaluation. Trente cas ont été planifiés avec et sans utilisation du modèle. La variabilité entre les opérateusrs a été évaluée par 12 opérateurs sur un cas. Les doses moyennes dans les glandes parotides (D_{moy}), l'indice d'homogénéité et le nombre d'unités moniteur (UM) ont été relevés.

Résultats : au total, 89 % des D_{moy} dans les glandes parotides prédites par le modèle ont été atteintes. L'utilisation du modèle a significativement réduit la D_{moy} dans les glandes parotides : -6,1 ± 4,3 Gy. Avec le modèle, une moins bonne homogénéité dans le PTV ainsi qu'une augmentation des UM (+10,5 % en moyenne) ont été obtenues. Pour la variabilité entre les opérateurs, les histogrammes dose-volume (HDV) des glanes parotides étaient significativement différents avec et sans utilisation du modèle ; l'écart type de la D_{moy} est passé de 2,2 Gy à 1,2 Gy et de 2,9 Gy à 0,8 Gy respectivement pour les glandes parotides homolatérale et controlatérale.

Conclusion : Lors d'une planification inverse en ORL, le modèle optimisé guide l'opérateur en fournissant une valeur de D_{moy} atteignable la plus faible possible pour les glandes parotides, permettant ainsi une diminution significative de la D_{moy} de -6,1 Gy. Cette méthode permet de réduire significativement la variabilité entre les patients et entre les opérateurs lors de la planification dosimétrique.

Mots clés : Planification dosimétrique ; prédiction de la dose ; VMAT ; contrôle qualité

Abstract

Purpose: To guide parotid gland (PG) sparing at the dose planning step, a specific model based on overlap between PTV and organ at risk (Moore et al.) was developed and evaluated for VMAT in head-and-neck (H&N) cancer radiotherapy.

Materials and methods: One hundred and sixty patients treated for locally advanced H&N cancer were included. A model optimization was first performed (20 patients) before a model evaluation (110 patients). Thirty cases were planned with and without the model to quantify the PG dose sparing. The inter-operator variability was evaluated on one case, planned by 12 operators with and without the model. The endpoints were PG mean dose (D_{mean}), PTV homogeneity and number of monitor units (MU).

Results: The PG D_{mean} predicted by the model was reached in 89% of cases. Using the model significantly reduced the PG D_{mean}: -6.1 ± 4.3 Gy. Plans with the model showed lower PTV dose homogeneity and more MUs (+10.5% on average). For the inter-operator variability, PG dose volume histograms without the optimized model were significantly different compared to those with the model; the D_{mean} standard deviation for the ipsilateral PG decreased from 2.2 Gy to 1.2 Gy. For the contralateral PG, this value decreased from 2.9 Gy to 0.8 Gy.

Conclusion: During the H&N inverse planning, the optimized model guides to the lowest PG achievable mean dose, allowing a significant PG mean dose reduction of -6.1 Gy. Integrating this method at the treatment planning step significantly reduced the inter-patient and inter-operator variabilities.

Keywords: Treatment planning; prediction dose; VMAT; quality control

Introduction

Intensity modulated radiotherapy (IMRT) is the standard treatment for head-and-neck (H&N) cancer, sparing the parotid glands (PGs) with sharp dose gradients, and thereby limiting xerostomia [1–3]. However, there is variability during the treatment planning optimization process depending on the clinical case complexity, treatment planning system (TPS), modulation degree, or operator experience. A dose planning only based on the standard dose recommendations does not provide the optimal treatment planning for every patient [4]. Since 2006, several studies have proposed dose and/or geometric indexes/tools based on their own experience to limit treatment planning variability [5–11]. In 2011, Moore et al. proposed a method based on a mathematical model to guide operators during the dose planning process about the compromise between the delivered dose to the target volume and the organ at risk (OAR) dose constraints [5]. The mathematical model (based on a knowledge of prior patients) allows prediction of the lowest achievable mean dose (D_{mean}) to an OAR knowing the prescribed dose to the PTV and the overlap volume between the PTV and considered OAR. Moreover, they shown that this method better saves healthy tissues while decreasing inter-operator variability. However, the proposed model was not specific for tumor localization, and was conceived as part of the specific practices from the authors' institution (Washington University School of Medicine, St Louis, MO). To our knowledge, this type of method has not been developed in another institution, with an optimized model for PG sparing during H&N

cancer radiotherapy. In addition, the inter-operator variability with the implementation of such a method has not been evaluated.

In the context of volumetric modulated arc therapy (VMAT) for H&N cancer radiotherapy, the objectives of this study were:

- to optimize the published model of Moore et al. [5] for PG dose sparing, with our institution practices
- to evaluate the optimized model's performance in a large cohort of patients
- to quantify the PG dose sparing with the use of the optimized model (compared to the standard approach)
- to evaluate inter-operator variability

Methods

Patient characteristics, image acquisition and delineation

A cohort of 160 consecutive patients with histologically confirmed locally advanced H&N squamous cell carcinoma treated from December 2015 to September 2017 was used for this study. All patients had bilateral cervical lymph node irradiation. Thirty-eight patients included in the first phase of the study (optimization and evaluation of the mode) had post-operative radiotherapy. Computed tomography (CT) contrast-enhanced images, indexed every 2-3 mm, were acquired, from the vertex to the carina (Brilliance, Big Bore, Philips, Netherlands). Target volume and OARs were delineated slice-by-slice on CT images. The gross tumor volume (GTV) was defined by clinical examination, CT, and FDG-PET scan. The GTV encompassed all visible and palpable primary and nodal disease. In post-operative cases, areas of involved margins or lymph node stations containing lymph nodes with extracapsular extension were considered to be at very high risk. High-risk clinical target volume (CTV) was defined as areas potentially containing

microscopic disease limited by anatomic barriers or by the GTV plus a 10 mm margin, when an anatomic barrier was not clearly identified (e.g., base of the tongue), or when the lymph node levels containing involved lymph nodes and neighbouring node levels were considered at risk of subclinical involvement greater than 15-20%. Low-risk CTV encompassed the remaining lymph node areas at risk of potential microscopic spreading greater than 5%. The PTV, designed to account for setup uncertainties, was defined using an additional margin of 5 mm. OARs included spinal cord, brainstem, mandible, larynx, bilateral inner ears, oesophagus, pharyngeal constrictors, oral cavity, contralateral PG (CPG), ipsilateral PG (IPG), and submandibular glands (SMGs). These OARs were delineated by radiotherapists regarding international recommendations [12]. The term ipsilateral or contralateral makes reference to the relationship between the OAR and the highest dose level PTV.

Dose planning

All patients received definitive or post-operative external beam radiotherapy using VMAT technique. Patients were immobilized in the supine position with custom aquaplast masks holding both the neck and shoulders (Posicast-Lite PR5, CIVCO, Iowa, US). Two or three dose levels in simultaneously integrated boost (SIB) were used, depending on the clinical situation (Table 1). Treatment planning was carried out on the Pinnacle v.9.10 (Philips) TPS using 6 MV photon beams from a Synergy or VERSA HD linear accelerator (Elekta, Stockholm, Sweden) equipped with an Agility (160 leafs) multileaf collimator. The collapsed cone convolution algorithm and a dose grid size of 3x3x3 mm^3 were used for dose calculation. Two 358° clockwise and counter-clockwise arcs (control point every 2°) were used. The highest priority was assigned to PTVs with the following constraints: more than 95% of any PTV should receive more than 95% of the prescribed dose, or more than 98% of any PTV should receive more than 90% of the prescribed dose; no more than 2%

of any PTV could receive more than 110%. The following OAR dose constraints were used [12–15]: brainstem and spinal cord maximum doses ($D_{2\%}$) were 50 Gy and 45 Gy, respectively; for the PG, the mean dose (D_{mean}) was <26 Gy or the maximum dose received by 50% of the volume was <30 Gy; for the SMG, D_{mean} was ≤39 Gy; for the oral cavity, D_{mean} was as low as possible; for the larynx, D_{mean} was ≤45 Gy; for the pharyngeal constrictors, D_{mean} was ≤40 Gy; for the oesophagus, Dmean was ≤35 Gy; for the internal and inner ears, $D_{2\%}$ was ≤40 Gy; and for the mandible, $D_{2\%}$ was ≤65 Gy.

All dose plans were performed by physicists or dosimetrists, and validated by a radiation oncologist.

Moore* et al. *optimization model

Moore et al. defined a mathematical model allowing for prediction of a radiation plan to achieve the lowest possible mean dose to an OAR [5]. This model depends on the prescribed dose to the PTV and the overlap volume between the PTV and considered OAR [5]. The equation of the model was the following:

$$\boldsymbol{D_{achievable_mean}} = \boldsymbol{D_{prescribed}}\left(\mathbf{A} + \mathbf{B}\left(\mathbf{C} - \boldsymbol{e}^{-\mathrm{D} \times \boldsymbol{V_{overlap}/V_{PG}}}\right)\right) \quad (\mathbf{1})$$

Voverlap is the intersection between PTV and PG.

This model was created from 17 H&N patients (overlap between PGs and PTV) and 8 prostate patients (overlap between rectum and prostate) static IMRT plans, with A = 0.2; B = 0.8; C = 1; D = 3.

An adapted Moore's model was fitted based on 20 H&N standard treatment plannings from our institution. A script was developed in the TPS to extract volumes of PTV, PGs and overlaps between PTV and each PG. Delivered mean doses to the PGs were collected. Using these data, the ratio of the PG D_{mean} to the prescription dose to PTV

($D_{prescribed}$) was plotted against the ratio of the overlap volume between PTV and PG ($V_{overlap}$) to the PG volume (V_{PG}), for each patient PG. Moore's equation coefficients (A, B, C and D) were modified by a dichotomy process, so that the curve of the model fits along the lower bound of our local data, representing the optimal average PG dose achievable in our selected cohort of patients (N = 20).

When the optimized model was used, the mean dose objective of the entire PG was adjusted in the TPS according to the Dachievable_mean (obtained from $D_{prescribed}$, $V_{overlap}$ and V_{PG}).

Evaluation of the optimized model (difference between the achievable PG mean dose calculated by the model and the planned PG mean dose)

The robustness of the adapted Moore model was assessed for a cohort of 110 H&N patients. Treatment plans were optimized knowing lowest achievable PG mean dose from the optimized model, from the equation (1). When the PG $D_{predicted}$ was not reached, an analysis was performed to understand the model limits.

Comparison between the standard planning and the use of the optimized model for achievable PG mean dose prediction

A comparison between the standard planning and the planning with the use of achievable PG mean doses was performed in a cohort of 30 H&N patients treated with definitive radiotherapy. Patients with post-operative irradiation were not included in this phase of the study to avoid biases in the data analysis. Dose planning was first performed with standard planning dose constraints [12–14]. Then, three planners retrospectively re-planed the 30 H&N cases using the lower achievable PG mean dose provided by the optimized model during the dose planning process.

Inter-operator variability with standard planning and the use of the optimized model for achievable PG mean dose prediction

The impact of the model application on inter-operator variability was evaluated in one H&N representative case of our clinical practices, with three dose levels (IPG overlap with PTV: 3.3 cm^3; CPG overlap with PTV: 1.7 cm^3). Twelve operators (medical physicists and dosimetrists) with different dosimetric experience (from 3 months to 10 years, median = 2.75 years) performed two plans of the same case: one with the standard planning and one using PG achievable mean dose provided by the optimized model.

Endpoints and statistical analysis

a. Dose endpoints

Dose distributions were assessed with dose volume histograms (DVHs) and particular dosimetric points, including the volume of the PTV receiving at least 95% of the prescribed dose ($V_{95\%}$), the mean dose to PG, and the maximum dose ($D_{2\%}$) to the spinal cord.

In addition, the delta index (δ) was computed to evaluate the ability of the model to be respected [5]. It was defined as:

$$\boldsymbol{\delta = \frac{D_{mean} - D_{predicted}}{D_{predicted}}} \qquad \mathbf{(2)}$$

Ideal δ value is 0 (no difference between mean doses predicted and planned). δ index allows to define the deviation between the predicted dose value by the model ($D_{predicted}$) and the final calculated dose ($D_{achieved}$).

NTCP values were calculated for PGs with the parameters defined by Dijkema et al. [16] and Houweling et al. [17]: TD50 = 39.9 Gy; n = 1; m = 0.40.

b. Treatment plan quality

Plans were assessed by conformity [18], and homogeneity [19] indexes, and complexity metrics. These indexes are defined as follows:

$$\boldsymbol{Conformity\ index\ (CI) = \frac{V_{PTV\ 95\%}}{V_{PTV}}} \quad (3)$$

where $V_{PTV95\%}$ is the volume of PTV receiving 95% of the prescribed dose. V_{PTV} is the volume of the PTV. Ideal CI value is 1.

$$\boldsymbol{Homogeneity\ index = \frac{D_{2\%} - D_{98\%}}{D_{50\%}}} \quad (4)$$

where $D_{2\%}$, $D_{98\%}$ and $D_{50\%}$ represent the doses to 2%, 98% and 50% of the PTV, respectively. Ideal HI value is 0.

Complexity of treatment plans was calculated with different metrics described by Du el al. [20]:

- number of monitor units (MU) planned (1 UM = 1 cGy in reference conditions: 10 cm x 10 cm square field, Skin Surface Distance = 95 cm, depth = 5 cm)
- aperture area (computed as the total area of all MLC segments openings, in cm^2)
- aperture irregularity (calculated the non-circularity of the aperture, equal to 1 in case of circular aperture)
- beam modulation (taking into account aperture area and MU number associated to each segment, equal to 0 with a treatment plan without modulation)

Quality assurance of treatment plans was performed with EBT3 Gafchromic films (Ashland) in an Octavius 40043-CT homogeneous phantom (PTW). Films were scanned using the Epson 11000XL desktop flat-bed scanner in association with FilmQAPro

software (Ashland). Comparison between delivered and calculated dose distributions was performed by local gamma analysis [21] (Verisoft software v7.0.1, PTW) with 3%/3 mm and 30% low dose threshold criteria.

c. Statistical analysis

Wilcoxon (non-parametric) tests were performed to compare standard planning with planning using the optimized model. A p-value ≤ 0.05 was considered as significant. Correlation test (Spearman) was performed between dose difference (optimized model minus standard method) and $V_{overlap}/V_{PG}$.

Results

Moore et al. *model optimization: determination of the minimum PG achievable mean dose*

Figure 1 displays the PG mean dose normalized to the prescribed doses for PTV in function of the relative overlap between PG and PTV. The mathematical model defined by equation (4) showed better fitting PG sparing considering overlap with the PTV and the prescribed dose to the PTV (solid curve in Fig. 1 representing the inferior shape).

$$\boldsymbol{D_{mean} = D_{prescribed}\left(0.17 + 0.8\left(1.02 - e^{-V_{overlap}/V_{PG}}\right)\right)} \quad (5)$$

where D_{mean} is the achievable PG mean dose, prescribed dose is the dose prescribed to the PTV, $V_{overlap}$ is the overlap volume between PG and PTV, and V_{PG} is the PG volume. Then, the D_{mean} provided by this optimized model for each PG was used during the planning process. These values were implemented as optimization goals with a script.

Evaluation of the optimized model (difference between the achievable PG mean dose calculated by the model and the planned PG mean dose)

Figure 2 displays the normalized mean doses ($D_{mean}/D_{prescribed}$) to PGs plotted against the ratio between volume overlap between the PTV and the PG, within a cohort of 110 patients.

The mean (± SD) δ index value was 0.13 (± 0.11) for the IPG and 0.9 (± 0.12) for the CPG. The δ index value of 26 PGs was outside the range [mean δ ± 1 SD], including 15 IPGs and 12 CPGs (circles in Figure 2).

Evaluation of PG sparing with the optimized model compared to the standard method

Figure 3 and Figure 4 presents the mean PTV and PG DVHs for treatment plans performed with and without the optimized model, within a cohort of 30 patients. Table 2 presents the delivered doses to PTVs and OARs, δ index and NTCP. Plans performed with the use of optimized model showed an increase of mean PTV coverage and an increase of PTV maximum dose (+1.1 Gy on average). On average, the IPG mean dose decreased of -6.4 Gy, and the CPG mean dose of -5.8 Gy. Mean doses were similar with standard planning for oral cavity and SMG ($p>0.05$) and significantly different for larynx and spinal cord ($D_{2\%}$), but accepted by physician. Using the optimized model on the PGs, δ index values were significantly lower and NTCP values significantly lower (p-value < 0.01).

Figure 5 displays box plots of the PG mean dose with the standard planning, the achievable PG mean dose predicted by the optimized model and the final PG mean dose reached using the optimized model. Dispersion (minimum value – maximum value) was larger with standard method than optimized one: 43.8 Gy versus 36 Gy for IPG and 35.8 Gy versus 28.6 Gy for CPG. Figure 6 shows "$D_{mean}/D_{prescription}$" plotted against

"$V_{overlap}/V_{PG}$" for the 20 patients for the IPG (Figure 6a.) and for the CPG (Figure 6b.) obtained with the optimized model strategy. "$D_{mean}/D_{prescription}$" plotted against "$V_{overlap}/V_{PG}$" for the standard planning has also been reported on Figure 6. No correlation (r_s (IPG) = 0.02 and r_s (CPG) = -0.46) was found between dose difference (optimized model minus standard method) and $V_{overlap}/V_{PG}$. Table 3 gathers also the conformity, homogeneity and complexity indexes and the results of agreement between TPS dose calculation and measurement. Plans performed with the optimized model were more heterogeneous for high- and middle-dose PTV than with standard planning. Plans performed with the optimized model were more complex than those performed with standard planning. In fact, significant smaller field sizes (mean of 50.1 cm² versus 56.8 cm² with standard planning) and significant MU increase (745 MU versus 673 MU with standard planning) were obtained with the use of the optimized model. Agreement between the TPS dose calculation and measurement was not significantly different between the planning methods.

Evaluation of inter-operator variability with standard planning and the use of the optimized model for achievable PG mean dose prediction

Figure 7 displays the minimum and maximum envelopes of the PG DVH for the H&N case planned by 12 different operators, with the standard planning (red colour) and with the use of optimized model (green colour). With the standard planning, the standard deviations of the PG mean doses were 2.2 Gy for the IPG and 2.9 Gy for the CPG. With the use of the optimized model the standard deviations significantly decreased to 1.2 Gy for the IPG and 0.8 Gy for the CPG. Table 4 shows the PTV CI and HI indexes. The PTV CI indexes were not significantly different between the standard planning and the use of the optimized

model. However, treatment plans performed with the optimized model provided HI indexes significantly higher for high and middle dose PTVs and not significantly different for low dose PTV.

Discussion

For H&N treatment planning, we showed the dosimetric benefit of using a simple, personalized and realistic model to predict achievable dose to the PGs. With this model, the PG mean doses decreased by 6.1 Gy on average compared to a standard planning, without compromising PTV coverage and without OAR overdose (Table 2). Moreover, the inter-operator variability was divided by 2 and by 3 for IPG and CPG mean doses, with the optimized model. In average, for standard method, IPG mean doses were above GORTEC recommendation (32.4 Gy for 26 Gy recommended) [12]. Using optimized method, mean IPG dose was equal to GORTEC recommendation. For CPG, optimized method reduced in average PG mean dose below GORTEC recommendation (26.9 Gy to 21 Gy).

PG mean doses obtained using the optimized model were consistent with Moore et al. [5] results. In their study, the model was applied to rectal and H&N IMRT cases. For H&N, the δ index varied from 0.28 +/- 0.24 without the model, to 0.13 +/- 0.10 with the model. In our study, for H&N VMAT cases, δ index varied from 0.42 +/- 0.28 to 0.09 +/- 0.14 (Table 2). This method seems useful for all localizations with overlap between the PTV and OARs requiring a dose compromise. Powis et al. [22] recently defined their own model based on Moore's method for rectum sparing in case of prostate VMAT.

Guidelines recommend to deliver a mean dose lower than 26 Gy to the CPG and as low as possible to the IPG [4]. The way to achieve these constraints is strongly dependant on operator experience, especially for the CPG. In this study, regardless of operator

experience, the inter-operator variability significantly decreased using the optimized model (Figure 7).

In this study, only 10% of 110 treatment plans realized with the optimized model were outside the arbitrary range [mean δ index ± 1 SD] (represented with points on Figure 2). Some cases could be explained both by the small overlap volume between PGs and PTV, and a PG location on the whole length close to the PTV. For such geometry, more sophisticated models might provide better dose prediction, as the overlap volume histogram (OVH) proposed by Wu et al. [7]. The OVH describes the fractional OAR volume that is within a specified distance to the PTV. This concept could be more suitable for non-overlapping cases but is more complex to implement in clinical routine. Another cause of deviation (between predicted and planned doses) can appear in case of PTV proximity to OAR requiring stringent dose constraints, such as brainstem or spinal cord.

We stress that implementation of such model must be institution-specific because TPS, treatment techniques, or OAR dose constraints can affect the performance of the model. Institution-specific trade-offs have also a major influence on the model. For now, we have only optimized the model for H&N VMAT treatment planning. Even in our institution, the model will need to be re-evaluated to be applied on another clinical localization or irradiation technique.

The optimized model used in this study increased the treatment plan complexity (Table 3). Improving PG sparing generated thinner and smaller segments and increased the number of MUs. Planners should be attentive to avoid too complex treatment plans, by using complexity index thresholds for example. Higher modulation complexity may result in lower dose accuracy. In that way, we performed quality controls to check the dose accuracy. Plans with the optimized model did not show significant difference (Table 3).

Our standard method did not provide any index to inform planner if the lowest OAR dose value is achieving, while covering PTV. Since several years, new automated planning tools were commercialized (AutoPlanning module for Pinnacle (Philips) TPS, RapidPlan for Varian TPS, etc.). Those tools can improve OAR sparing and/or PTV coverage, especially for new planners [23]. Implementation of such tools, needs time to be configured (especially for knowledge-based methods) and evaluated to be confident with. Several studies evaluated the impact of those commercial solutions on PG sparing [23–26]. Compared to manual planning, the use of RapidPlan in a H&N study including 20 patients, allowed a mean PG decrease of 2.2 Gy [24]. With AutoPlanning software, a H&N study on 10 patients reported on average a PG mean dose decrease of 3 Gy [25], and another study on 10 patients found a PG mean dose reduction of 1.5 Gy [23]. Such tools appear attractive but are always a TPS add-on with additional cost. Our implementation of optimized model required only methodology and time. The two approaches, commercial tool and optimized model, are not rivals and can be implemented together [26,27].

Mean dose PG sparing is a crucial objective for H&N IMRT/VMAT techniques. Indeed, due to large anatomical variations during treatment course, the delivered dose may differ from the initial planned dose, especially a dose increase for the PGs [28–30]. Adaptive radiotherapy (ART), using one or several replannings [31,32], has been proposed to spare the PGs [33–37]. Weekly replannings can reduce the PG mean dose by 5 Gy, translating a reduction of 11% in the NTCP risk for xerostomia [30]. Thus, ART workflow can provide PG dose sparing and clinical benefit for some patients (30 to 65% of patients [29]). However, it was known as very time consuming and requiring resources strategy. In this context, the integration of an adapted Moore's method to local dosimetric protocols could reduce PG mean dose easier than an ART strategy.

This study has some limitations. In the model optimization and robustness phase of this work, 38 patients with post-operative bilateral neck irradiation were included to reflect our institutional daily practice. However, in the comparison phase (optimized model versus standard method) only patients with radical radiotherapy were included to avoid biases in the data analysis. Because the achievable lowest dose delivered to the PGs are driven by the prescribed dose to the PTV and the $V_{overlap}$ between this PTV and the PG, we may assume that the results obtained for patients with radical radiotherapy would be similar to those with the post-operative radiotherapy. Indeed, our radical radiotherapy protocol include dose levels quite similar to our post-operative protocol for the high risk and elective target volumes. The optimized model was based on a cohort of 20 patients and would likely be more robust with a larger cohort, including more complex geometries to improve the dose prediction of non-standard cases. The inter-operator variability was assessed only on one case, and could be extended on more clinical cases. As using the optimized model increases treatment plan complexity, a constraint in term of minimum segment area or maximum MU could have been introduced. Moreover, this study could be supplemented by a multi-centric study to extent methodology to other practices.

Conclusions

A simple and optimized mathematical model was implemented in our department to spare the PGs during H&N treatment dose planning. Using the achievable PG mean dose provided by the optimized model, the PG mean dose decreased of 6.1 Gy on average. Moreover, the optimized model allows to significantly reduce the inter-operator variability, whatever the planner's experience. The optimized model has been used in our daily clinical practices for the last two years. The benefits of PG dose sparing need to be evaluated in terms of clinical benefits (e.g., xerostomia, local control).

References

[1] Kam MKM, Leung S-F, Zee B, Chau RMC, Suen JJS, Mo F, et al. Prospective Randomized Study of Intensity-Modulated Radiotherapy on Salivary Gland Function in Early-Stage Nasopharyngeal Carcinoma Patients. Journal of Clinical Oncology 2007;25:4873–9. doi:10.1200/JCO.2007.11.5501.

[2] Feng FY, Kim HM, Lyden TH, Haxer MJ, Worden FP, Feng M, et al. Intensity-Modulated Chemoradiotherapy Aiming to Reduce Dysphagia in Patients With Oropharyngeal Cancer: Clinical and Functional Results. Journal of Clinical Oncology 2010;28:2732–8. doi:10.1200/JCO.2009.24.6199.

[3] Pow EHN, Kwong DLW, McMillan AS, Wong MCM, Sham JST, Leung LHT, et al. Xerostomia and quality of life after intensity-modulated radiotherapy vs. conventional radiotherapy for early-stage nasopharyngeal carcinoma: Initial report on a randomized controlled clinical trial. International Journal of Radiation Oncology*Biology*Physics 2006;66:981–91. doi:10.1016/j.ijrobp.2006.06.013.

[4] Bentzen SM, Constine LS, Deasy JO, Eisbruch A, Jackson A, Marks LB, et al. Quantitative Analyses of Normal Tissue Effects in the Clinic (QUANTEC): An Introduction to the Scientific Issues. International Journal of Radiation Oncology*Biology*Physics 2010;76:S3–9. doi:10.1016/j.ijrobp.2009.09.040.

[5] Moore KL, Brame RS, Low DA, Mutic S. Experience-Based Quality Control of Clinical Intensity-Modulated Radiotherapy Planning. International Journal of Radiation Oncology*Biology*Physics 2011;81:545–51. doi:10.1016/j.ijrobp.2010.11.030.

[6] Hunt MA, Jackson A, Narayana A, Lee N. Geometric factors influencing dosimetric sparing of the parotid glands using IMRT. International Journal of Radiation Oncology*Biology*Physics 2006;66:296–304. doi:10.1016/j.ijrobp.2006.05.028.

[7] Wu B, Ricchetti F, Sanguineti G, Kazhdan M, Simari P, Chuang M, et al. Patient geometry-driven information retrieval for IMRT treatment plan quality control. Medical Physics 2009;36:5497–505. doi:10.1118/1.3253464.

[8] Mattes MD, Lee JC, Elnaiem S, Guirguis A, Ikoro NC, Ashamalla H. A predictive model to guide management of the overlap region between target volume and organs at risk in prostate cancer volumetric modulated arc therapy. Radiation Oncology Journal 2014;32:23. doi:10.3857/roj.2014.32.1.23.

[9] Stanhope C, Wu QJ, Yuan L, Liu J, Hood R, Yin F-F, et al. Utilizing knowledge from prior plans in the evaluation of quality assurance. Physics in Medicine and Biology 2015;60:4873–91. doi:10.1088/0031-9155/60/12/4873.

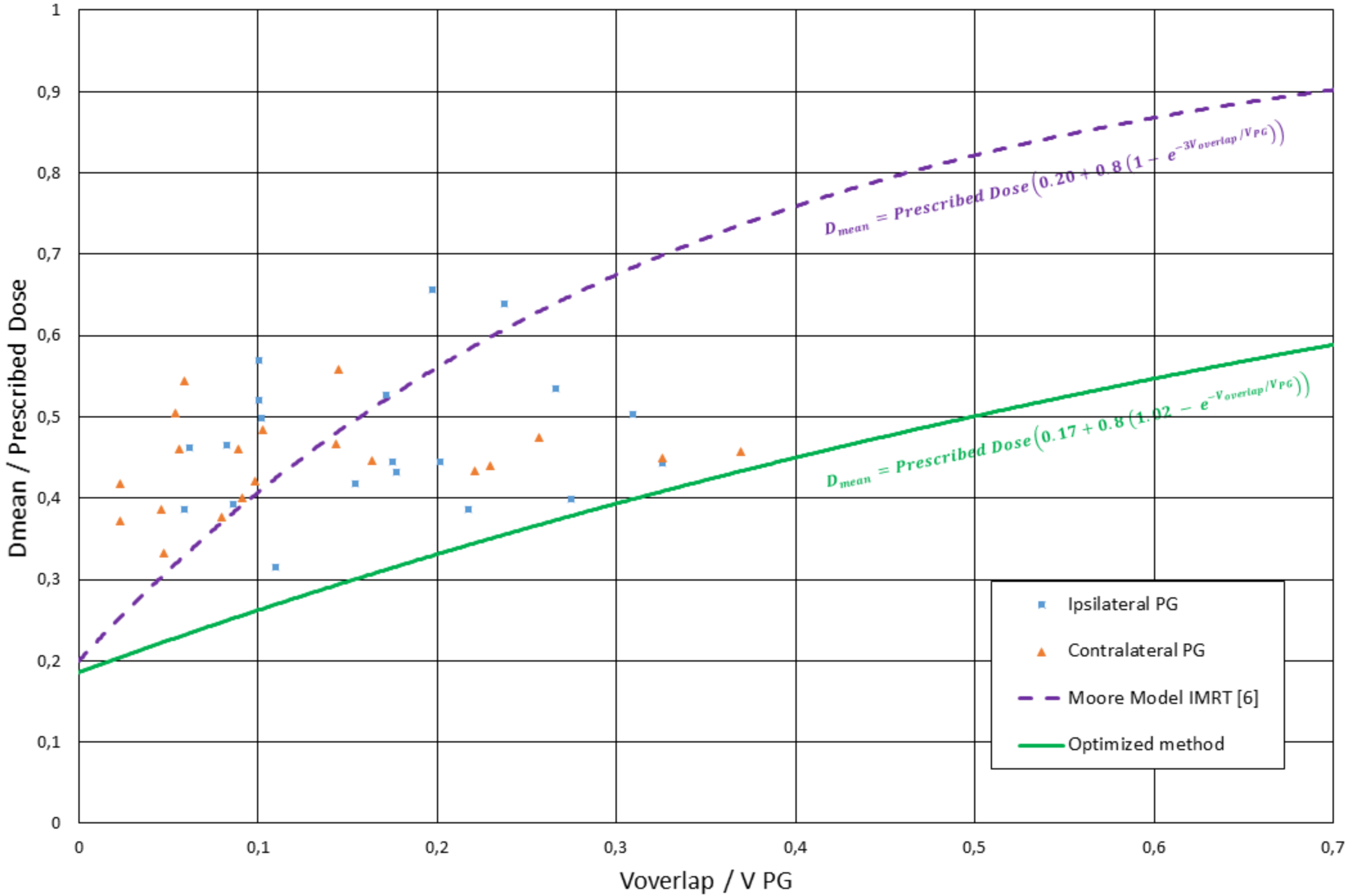
[10] Lian J, Yuan L, Ge Y, Chera BS, Yoo DP, Chang S, et al. Modeling the dosimetry of organ-at-risk in head and neck IMRT planning: An intertechnique and interinstitutional study: IMRT intertechnique and interinstitutional modeling. Medical Physics 2013;40:121704. doi:10.1118/1.4828788.

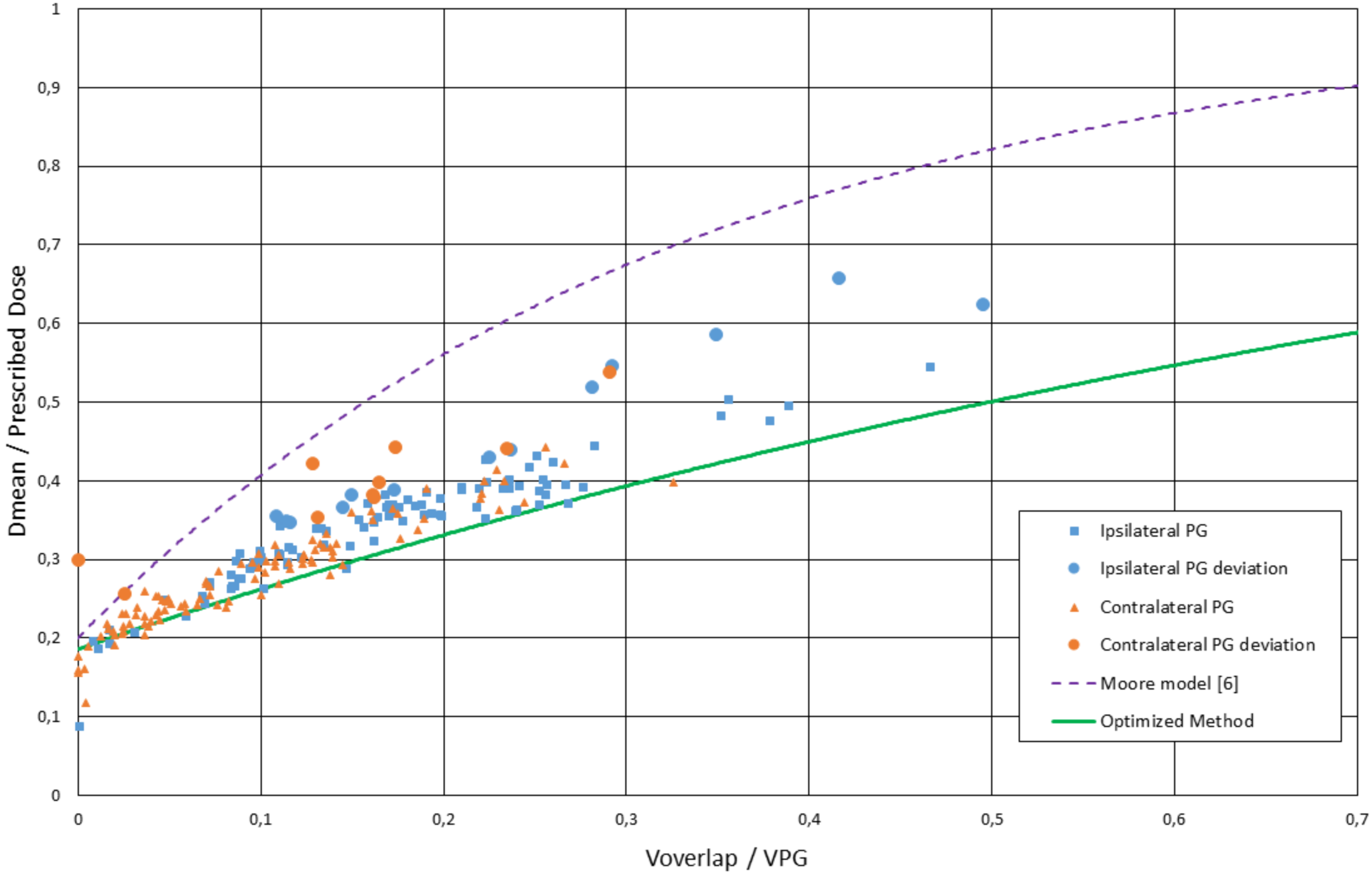
[11] Tol JP, Dahele M, Delaney AR, Slotman BJ, Verbakel WFAR. Can knowledge-based DVH predictions be used for automated, individualized quality assurance of radiotherapy treatment plans? Radiation Oncology 2015;10. doi:10.1186/s13014-015-0542-1.

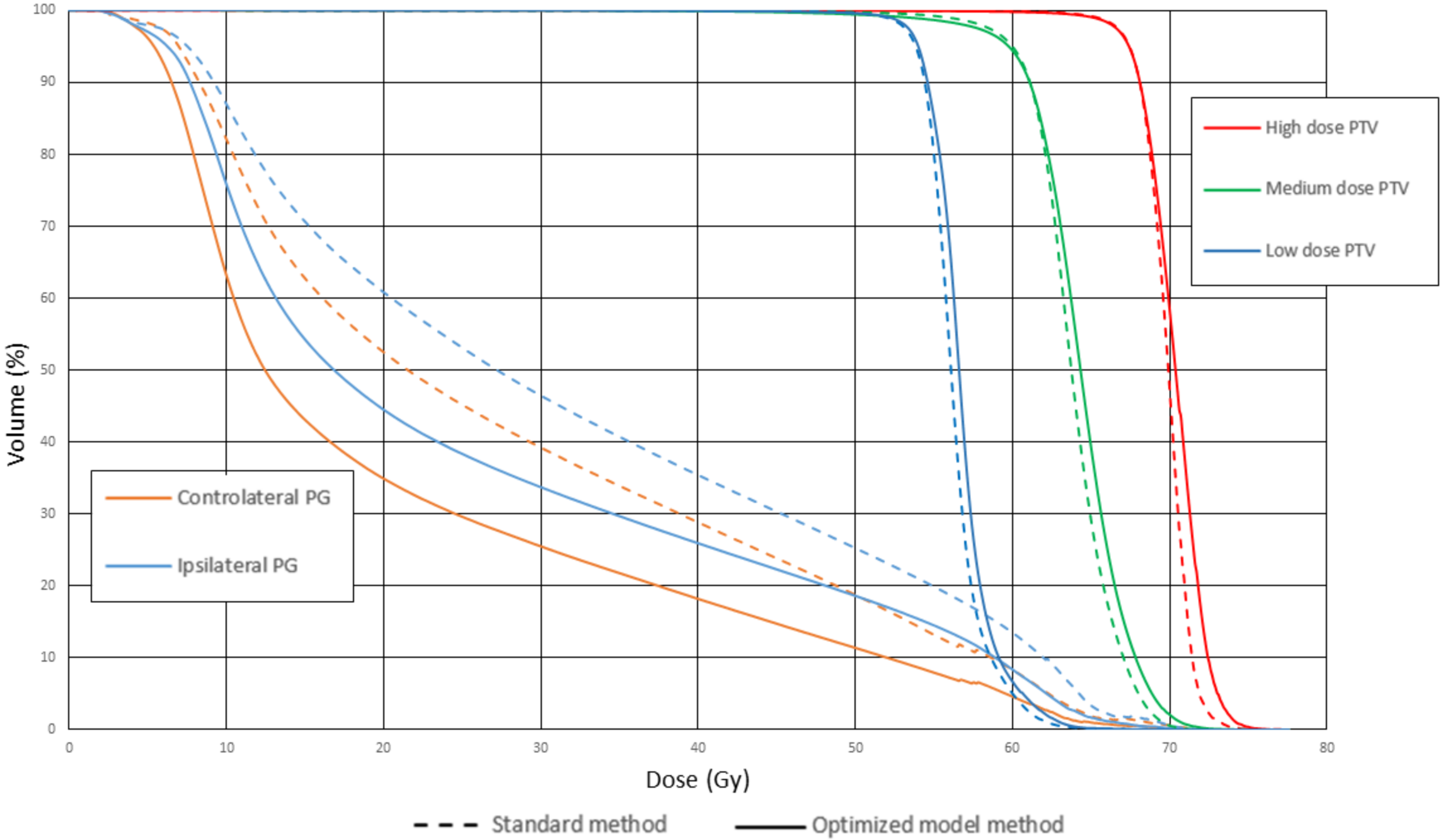
[12] Brouwer CL, Steenbakkers RJHM, Bourhis J, Budach W, Grau C, Grégoire V, et al. CT-based delineation of organs at risk in the head and neck region: DAHANCA, EORTC, GORTEC, HKNPCSG, NCIC CTG, NCRI, NRG Oncology and TROG consensus guidelines. Radiotherapy and Oncology 2015;117:83–90. doi:10.1016/j.radonc.2015.07.041.

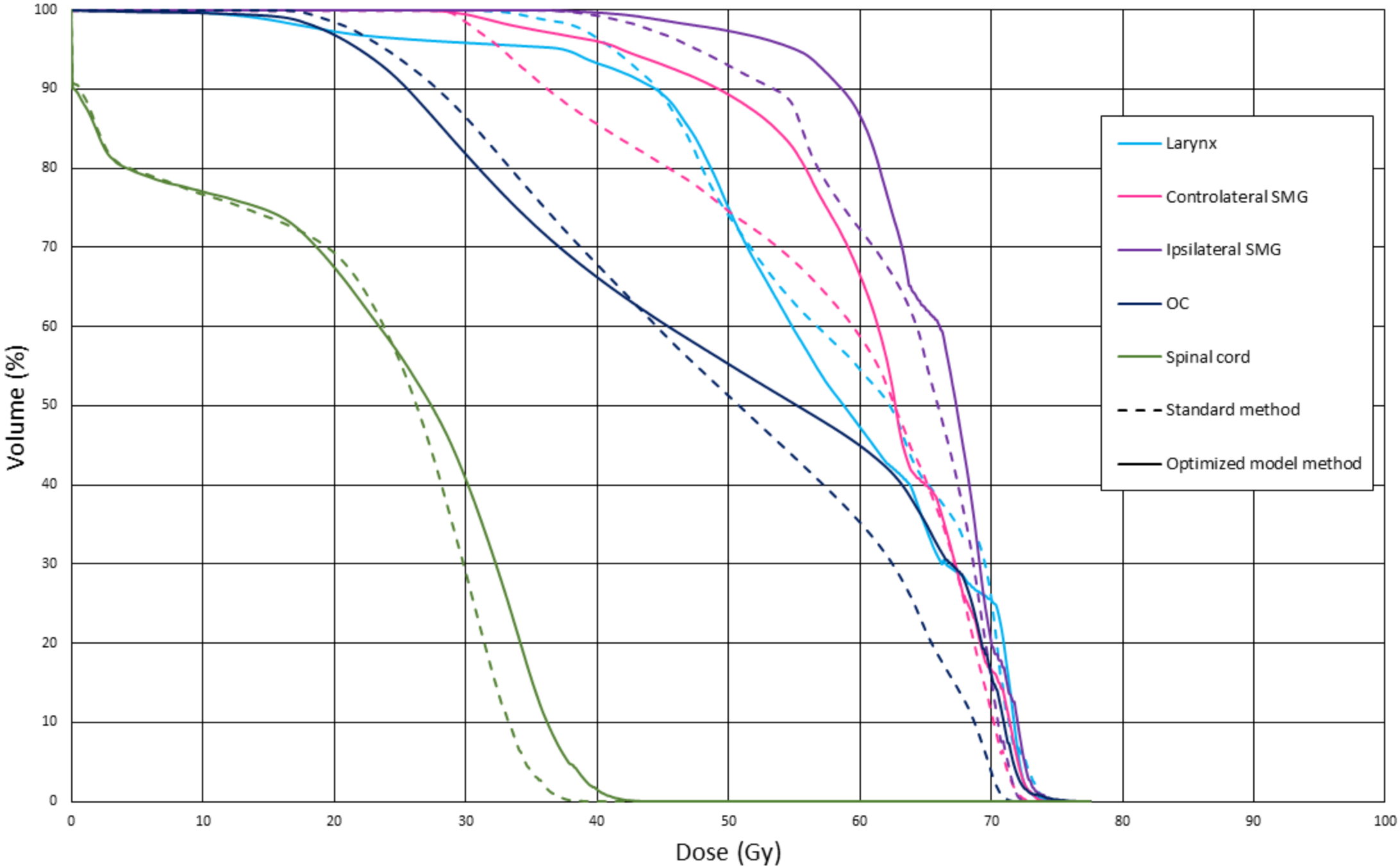
[13] Lee N, Chuang C, Quivey JM, Phillips TL, Akazawa P, Verhey LJ, et al. Skin toxicity due to intensity-modulated radiotherapy for head-and-neck carcinoma. International Journal of Radiation Oncology* Biology* Physics 2002;53:630–637.
[14] Maingon P, Giraud P, Pointreau Y. Chapitre commun à la prise en charge et à la procédure de préparation des traitements des cancers de la tête et du cou. Cancer/Radiothérapie 2016;20:S96–8. doi:10.1016/j.canrad.2016.07.001.
[15] Toledano I, Graff P, Serre A, Boisselier P, Bensadoun R-J, Ortholan C, et al. Intensity-modulated radiotherapy in head and neck cancer: Results of the prospective study GORTEC 2004–03. Radiotherapy and Oncology 2012;103:57–62. doi:10.1016/j.radonc.2011.12.010.
[16] Dijkema T, Raaijmakers CPJ, Ten Haken RK, Roesink JM, Braam PM, Houweling AC, et al. Parotid Gland Function After Radiotherapy: The Combined Michigan and Utrecht Experience. International Journal of Radiation Oncology*Biology*Physics 2010;78:449–53. doi:10.1016/j.ijrobp.2009.07.1708.
[17] Houweling AC, Philippens MEP, Dijkema T, Roesink JM, Terhaard CHJ, Schilstra C, et al. A Comparison of Dose–Response Models for the Parotid Gland in a Large Group of Head-and-Neck Cancer Patients. International Journal of Radiation Oncology*Biology*Physics 2010;76:1259–65. doi:10.1016/j.ijrobp.2009.07.1685.
[18] Lomax NJ, Scheib SG. Quantifying the degree of conformity in radiosurgery treatment planning. International Journal of Radiation Oncology*Biology*Physics 2003;55:1409–19. doi:10.1016/S0360-3016(02)04599-6.
[19] ICRU. Prescribing, Recording, and Reporting Photon-Beam Intensity-Modulated Radiation Therapy (IMRT). Journal of the ICRU 2010;10:NP.2-NP. doi:10.1093/jicru/ndq001.
[20] Du W, Cho SH, Zhang X, Hoffman KE, Kudchadker RJ. Quantification of beam complexity in intensity-modulated radiation therapy treatment plans. Medical Physics 2014;41.
[21] Low DA, Harms WB, Mutic S, Purdy JA. A technique for the quantitative evaluation of dose distributions. Medical Physics 1998;25:656–661.
[22] Powis R, Bird A, Brennan M, Hinks S, Newman H, Reed K, et al. Clinical implementation of a knowledge based planning tool for prostate VMAT. Radiation Oncology 2017;12. doi:10.1186/s13014-017-0814-z.
[23] Speer S, Klein A, Kober L, Weiss A, Yohannes I, Bert C. Automation of radiation treatment planning: Evaluation of head and neck cancer patient plans created by the Pinnacle3 scripting and Auto-Planning functions. Strahlentherapie Und Onkologie 2017;193:656–65. doi:10.1007/s00066-017-1150-9.
[24] Fogliata A, Reggiori G, Stravato A, Lobefalo F, Franzese C, Franceschini D, et al. RapidPlan head and neck model: the objectives and possible clinical benefit. Radiation Oncology 2017;12. doi:10.1186/s13014-017-0808-x.
[25] Gintz D, Latifi K, Caudell J, Nelms B, Zhang G, Moros E, et al. Initial evaluation of automated treatment planning software. Journal of Applied Clinical Medical Physics 2016;17:331–46. doi:10.1120/jacmp.v17i3.6167.
[26] Ge Y, Wu QJ. Knowledge-based planning for intensity-modulated radiation therapy: A review of data-driven approaches. Medical Physics 2019. doi:10.1002/mp.13526.
[27] Moore KL. Automated Radiotherapy Treatment Planning. Seminars in Radiation Oncology 2019;29:209–18. doi:10.1016/j.semradonc.2019.02.003.
[28] Brouwer CL, Steenbakkers RJHM, Langendijk JA, Sijtsema NM. Identifying patients who may benefit from adaptive radiotherapy: Does the literature on anatomic and dosimetric changes in head and neck organs at risk during radiotherapy provide

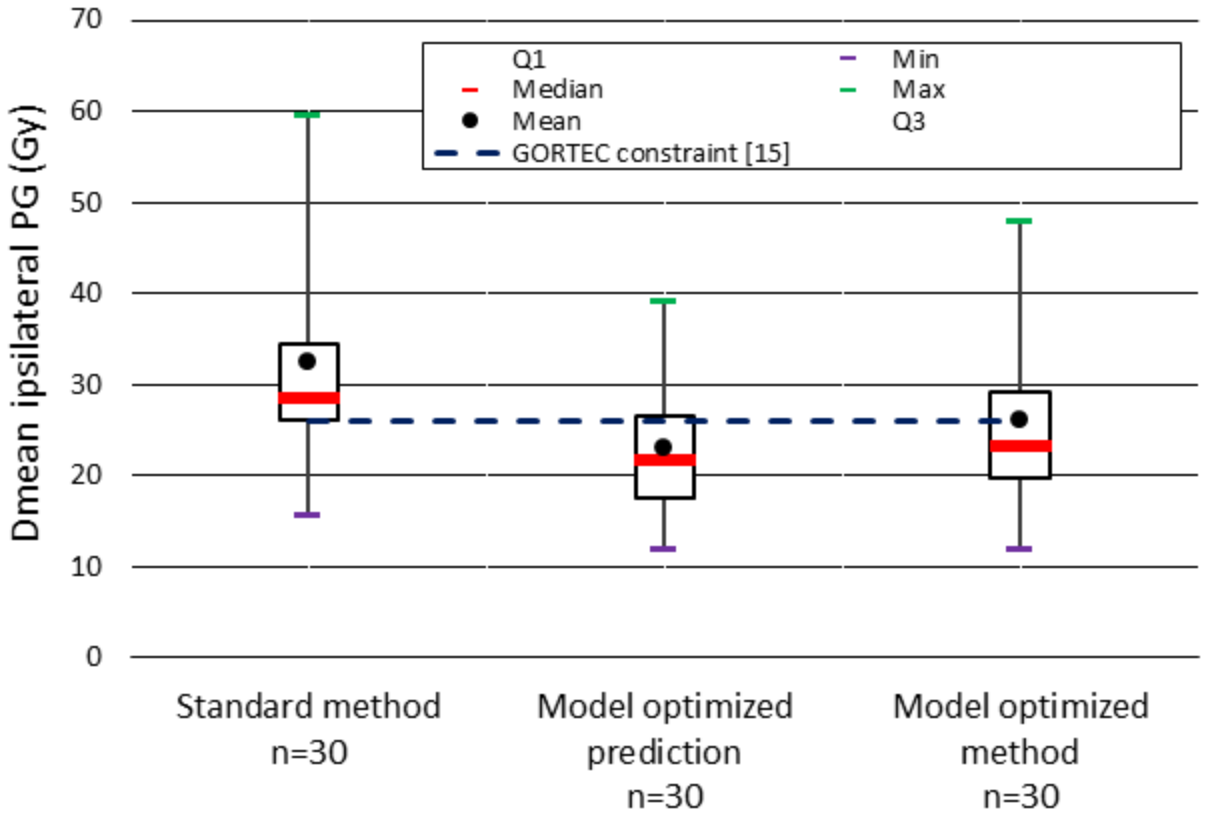
information to help? Radiotherapy and Oncology 2015;115:285–94. doi:10.1016/j.radonc.2015.05.018.
[29] Castelli J, Simon A, Lafond C, Perichon N, Rigaud B, Chajon E, et al. Adaptive radiotherapy for head and neck cancer. Acta Oncologica 2018;57:1284–92. doi:10.1080/0284186X.2018.1505053.
[30] Castelli J, Simon A, Louvel G, Henry O, Chajon E, Nassef M, et al. Impact of head and neck cancer adaptive radiotherapy to spare the parotid glands and decrease the risk of xerostomia. Radiation Oncology 2015;10:6. doi:10.1186/s13014-014-0318-z.
[31] Graff P, Huger S, Kirby N, Pouliot J. Radiothérapie adaptative ORL. Cancer/Radiothérapie 2013;17:513–22. doi:10.1016/j.canrad.2013.06.040.
[32] Heukelom J, Fuller CD. Head and Neck Cancer Adaptive Radiation Therapy (ART): Conceptual Considerations for the Informed Clinician. Seminars in Radiation Oncology 2019;29:258–73. doi:10.1016/j.semradonc.2019.02.008.
[33] Schwartz DL, Garden AS, Shah SJ, Chronowski G, Sejpal S, Rosenthal DI, et al. Adaptive radiotherapy for head and neck cancer—Dosimetric results from a prospective clinical trial. Radiotherapy and Oncology 2013;106:80–4. doi:10.1016/j.radonc.2012.10.010.
[34] Dewan A, Sharma S, Dewan A, Srivastava H, Rawat S, Kakria A, et al. Impact of Adaptive Radiotherapy on Locally Advanced Head and Neck Cancer - A Dosimetric and Volumetric Study. Asian Pacific Journal of Cancer Prevention 2016;17:985–92. doi:10.7314/APJCP.2016.17.3.985.
[35] Capelle L, Mackenzie M, Field C, Parliament M, Ghosh S, Scrimger R. Adaptive Radiotherapy Using Helical Tomotherapy for Head and Neck Cancer in Definitive and Postoperative Settings: Initial Results. Clinical Oncology 2012;24:208–15. doi:10.1016/j.clon.2011.11.005.
[36] Jensen AD, Nill S, Huber PE, Bendl R, Debus J, Münter MW. A Clinical Concept for Interfractional Adaptive Radiation Therapy in the Treatment of Head and Neck Cancer. International Journal of Radiation Oncology*Biology*Physics 2012;82:590–6. doi:10.1016/j.ijrobp.2010.10.072.
[37] Olteanu LAM, Berwouts D, Madani I, De Gersem W, Vercauteren T, Duprez F, et al. Comparative dosimetry of three-phase adaptive and non-adaptive dose-painting IMRT for head-and-neck cancer. Radiotherapy and Oncology 2014;111:348–53. doi:10.1016/j.radonc.2014.02.017.

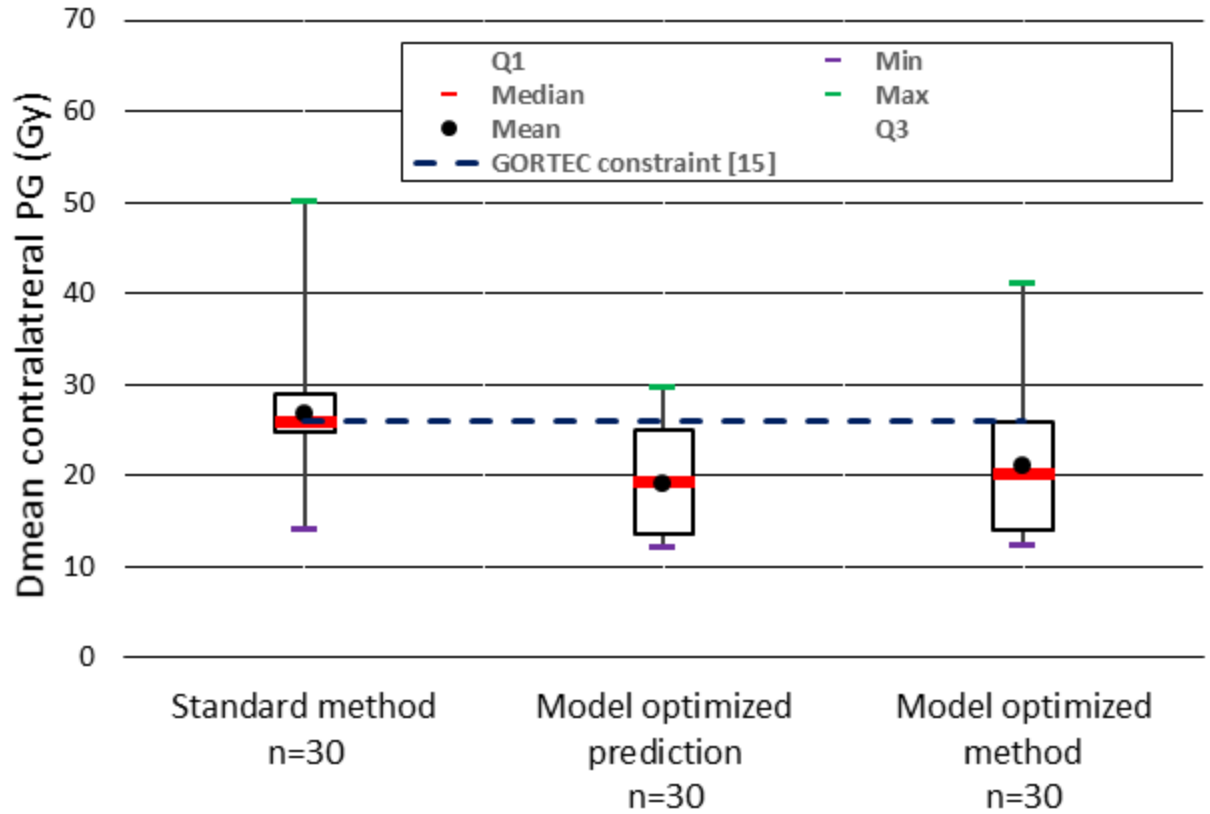

Dmean / Prescribed Dose
Voverlap / V PG
1
0,9
0,8
0,7
0,6
0,5
0,4
0,3
0,2
0,1
0
0
0,1
0,2
0,3
0,4
0,5
0,6
0,7
$D_{mean} = Prescribed\ Dose\left(0.20 + 0.8\left(1 - e^{-3V_{overlap}/V_{PG}}\right)\right)$
$D_{mean} = Prescribed\ Dose\left(0.17 + 0.8\left(1.02 - e^{-V_{overlap}/V_{PG}}\right)\right)$
Ipsilateral PG
Contralateral PG
Moore Model IMRT [6]
Optimized method


Dmean / Prescribed Dose
Voverlap / VPG
0
0,1
0,2
0,3
0,4
0,5
0,6
0,7
0,8
0,9
1
Ipsilateral PG
Ipsilateral PG deviation
Contralateral PG
Contralateral PG deviation
Moore model [6]
Optimized Method

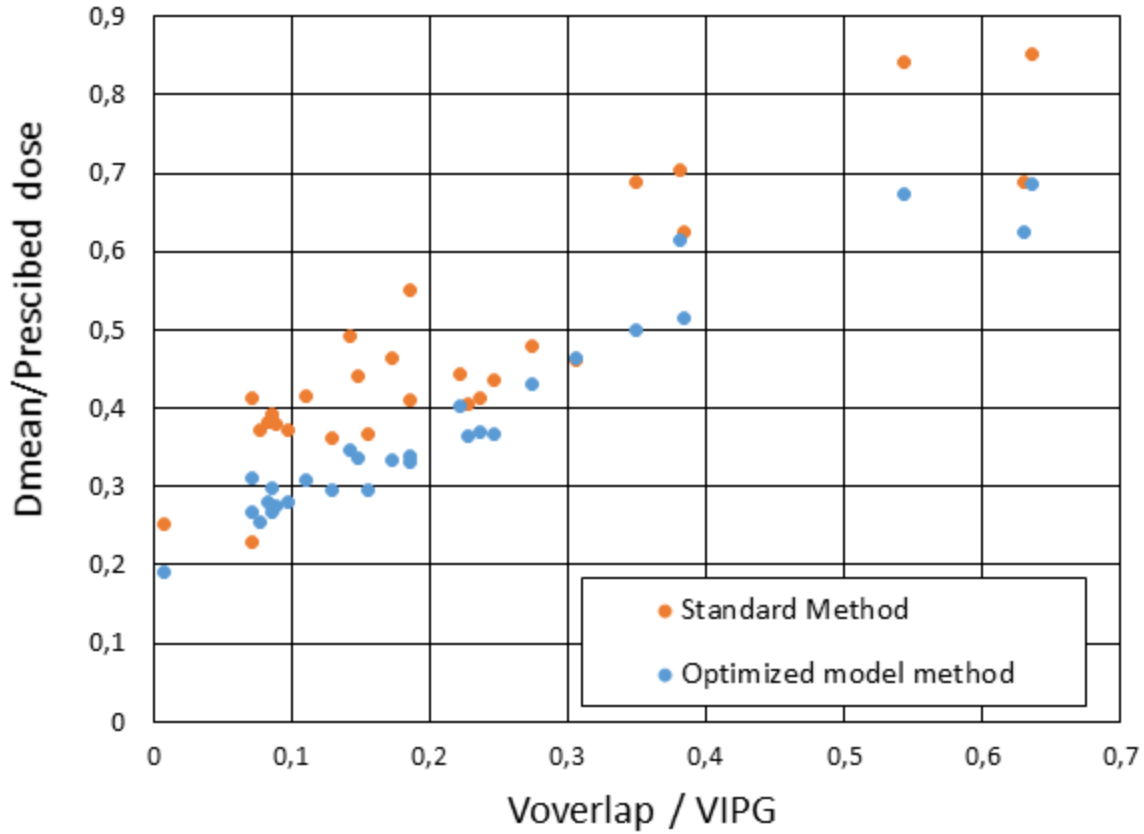

Volume (%)
Dose (Gy)
High dose PTV
Medium dose PTV
Low dose PTV
Controlateral PG
Ipsilateral PG
Standard method
Optimized model method


Volume (%)
Dose (Gy)
0
10
20
30
40
50
60
70
80
90
100
Larynx
Controlateral SMG
Ipsilateral SMG
OC
Spinal cord
Standard method
Optimized model method

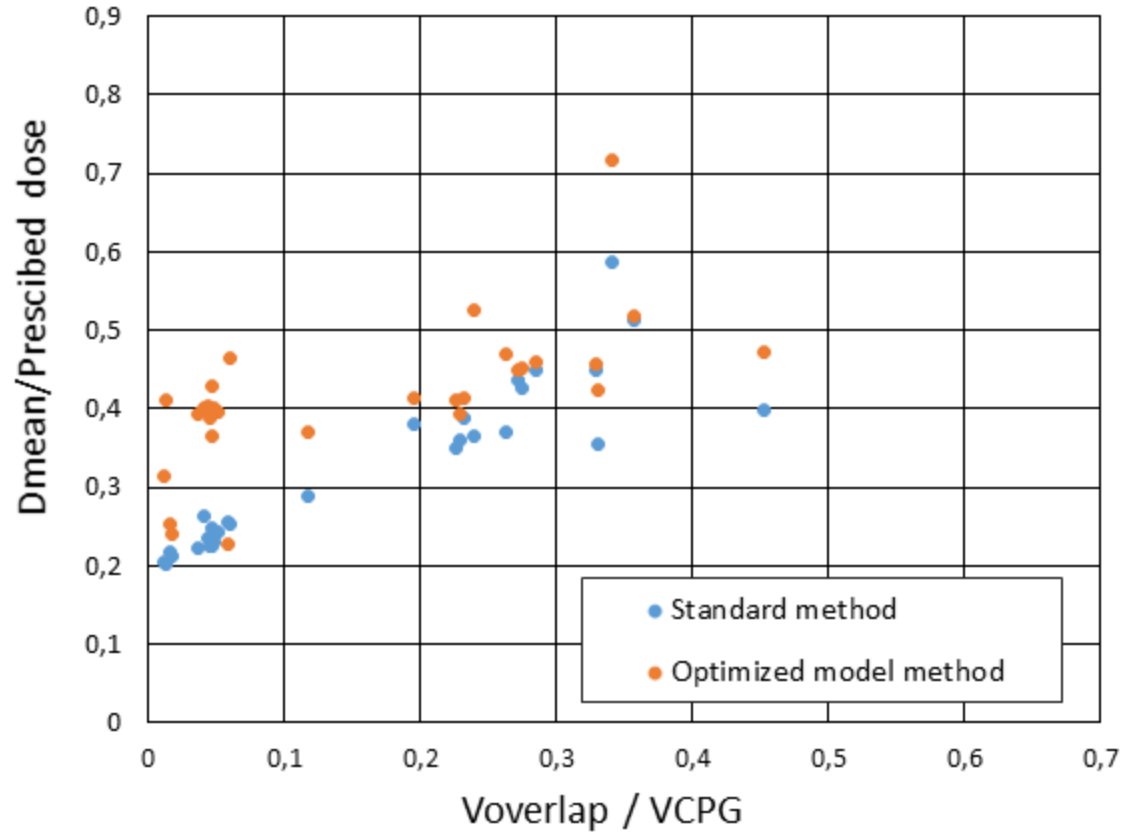

Dmean ipsilateral PG (Gy)
70
60
50
40
30
20
10
0
Q1
Median
Mean
GORTEC constraint [15]
Min
Max
Q3
Standard method n=30
Model optimized prediction n=30
Model optimized method n=30

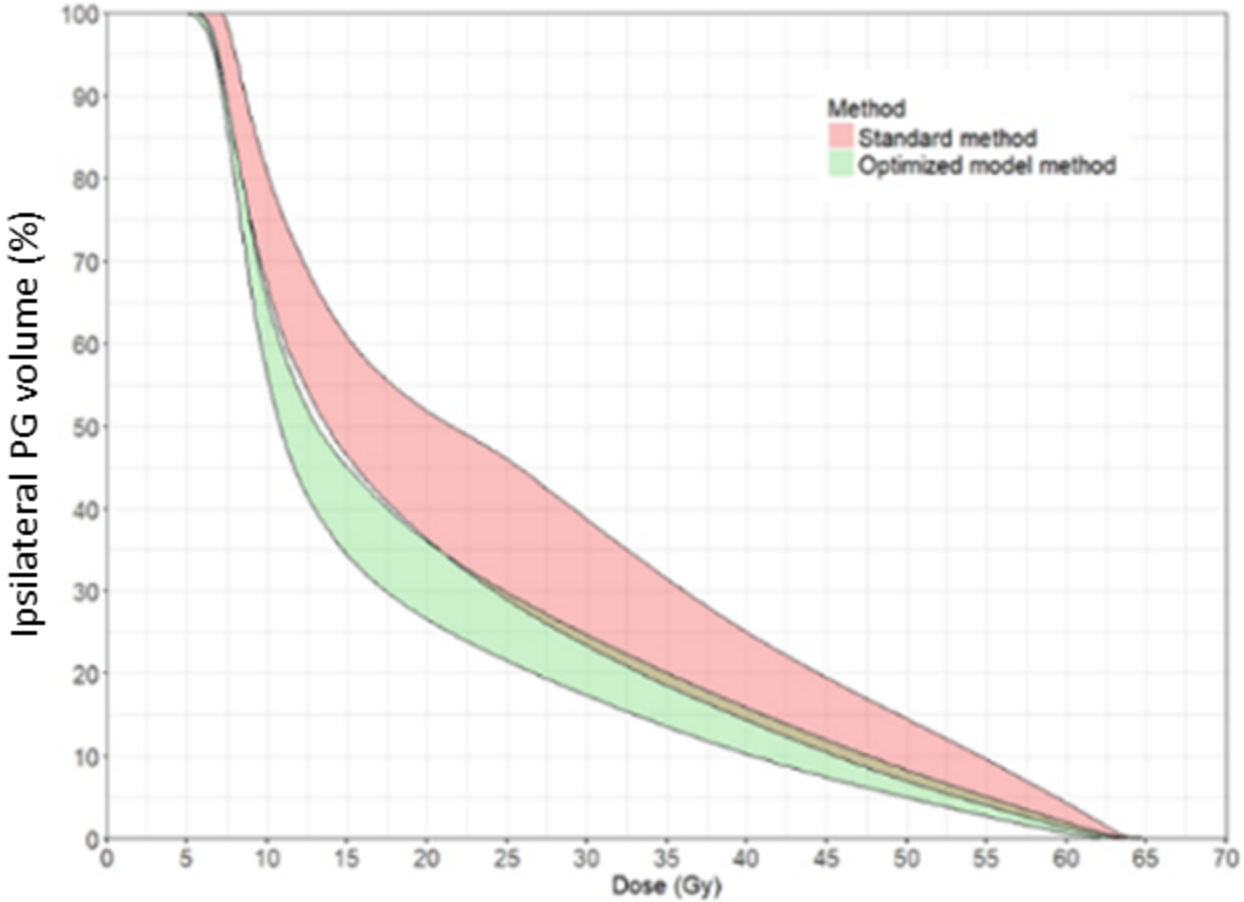

Dmean contralatreral PG (Gy)
70
60
50
40
30
20
10
0
Q1
Median
Mean
GORTEC constraint [15]
Min
Max
Q3
Standard method n=30
Model optimized prediction n=30
Model optimized method n=30

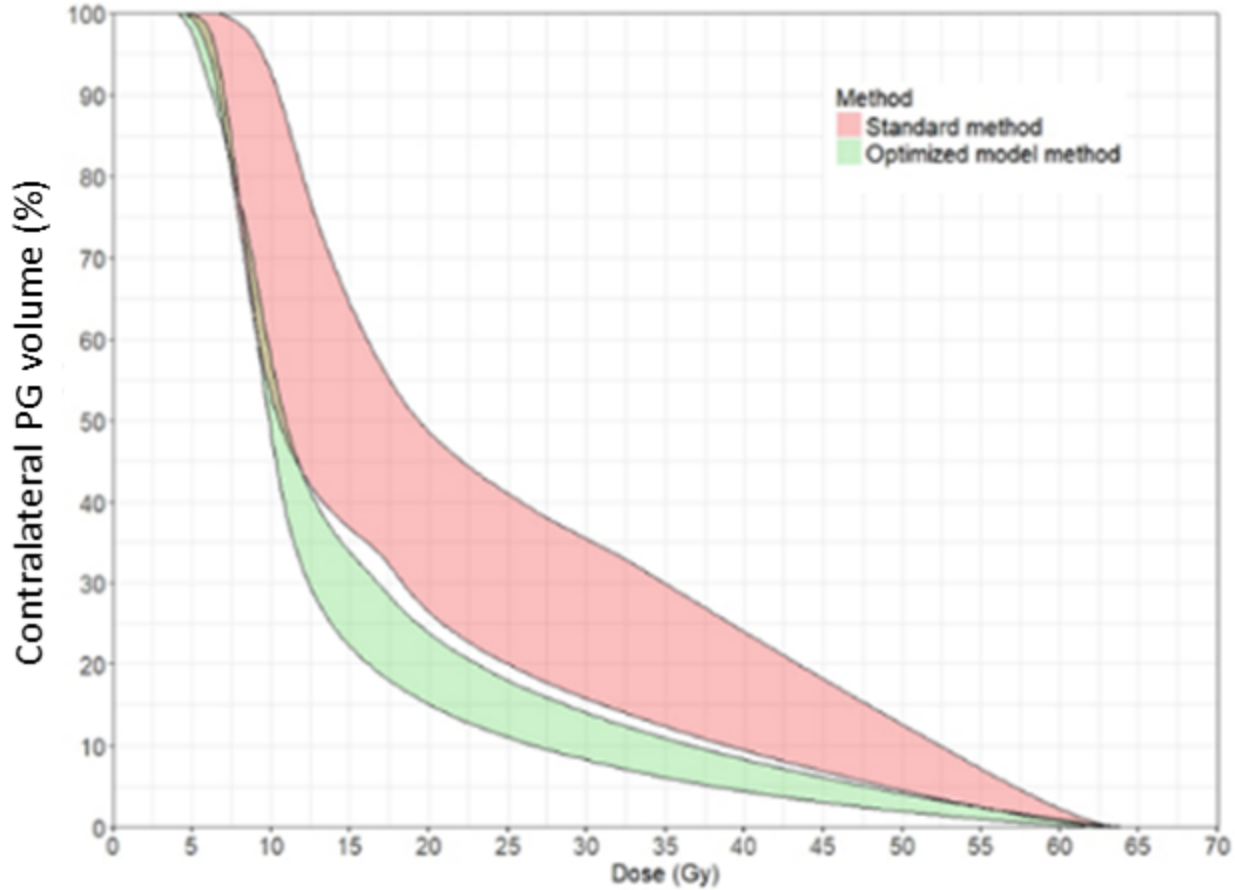
a/


Dmean/Prescibed dose
0,9
0,8
0,7
0,6
0,5
0,4
0,3
0,2
0,1
0
0
0,1
0,2
0,3
0,4
0,5
0,6
0,7
Voverlap / VIPG
Standard Method
Optimized model method

b/


Dmean/Prescibed dose
0,9
0,8
0,7
0,6
0,5
0,4
0,3
0,2
0,1
0
0
0,1
0,2
0,3
0,4
0,5
0,6
0,7
Voverlap / VCPG
Standard method
Optimized model method


Ipsilateral PG volume (%)
Dose (Gy)
Method
Standard method
Optimized model method


Contralateral PG volume (%)
Dose (Gy)
Method
Standard method
Optimized model method

	Cohort size (number of patients)	Dose prescription (number of patients)			PG volume (mean ± SD, in cm^3)		PG overlap (mean ± SD, in cm^3)	
		70–63-56 Gy	**66-59.4–54.1 Gy**	**60–54 Gy**	**IPG**	**CPG**	**IPG**	**CPG**
Model optimization	20	10	4	6	28.9 ± 10.2	29.1 ± 9.3	4.8 ± 2.6	3.4 ± 2.1
Robustness	110	82	20	8	29.6 ± 8.0	30.3 ± 9.1	5.0 ± 3.0	3.0 ± 2.1
Standard vs optimized model	30	30	0	0	27.5 ± 10.7	26.1 ± 11.0	4.9 ± 3.0	3.0 ± 1.9
Total	160	122	24	14	29.1 ± 8.1	29.4 ± 9.6	4.9 ± 2.9	3.1 ± 2.1

Table 1. Patient's study characteristics: patient cohort size, dose prescription, PG volume and, overlap between PG and PTV

IPG: ipsilateral parotid gland

CPG: contralateral parotid gland

		Standard planning Mean [min; max]	**With optimized model** Mean [min; max]	**p-value**
Planned dose to PTVs and OARs (in Gy)	High-dose PTV (D_{mean})	**69.8** [67.9; 71.8]	**70.1** [67.6;71.8]	**0.11**
	Middle-dose PTV (D_{mean})	**62.7** [62.1; 65.1]	**63.1** [61.2;65.9]	**0.03**
	Low-dose PTV (D_{mean})	**56.3** [54.6; 57.5]	**56.7** [54.8; 57.9]	**0.02**
	Spinal Cord ($D_{2\%}$)	**34.6** [30.6; 37.5]	**38.1** [34.7; 41.7]	**<0.001**
	Oral cavity (D_{mean})	**54.9** [26.8 ; 67.7]	**54.2** [28.7; 66.7]	**0.09**
	Larynx (D_{mean})	**56.7** [21.1; 83.2]	**57.2** [23.6; 71.8]	**0.03**
	Ipsilateral SMG (D_{mean})	**63.0** [33.3; 70.8]	**61.9** [37.9; 72.2]	**0.41**
	Contralateral SMG (D_{mean})	**57.9** [31.3; 71.1]	**58.6** [32.8; 71.7]	**0.18**
	Ipsilateral PG (D_{mean})	**32.4** [15.9; 59.7]	**26.0** [12.0; 48.0]	**<0.001**
	Contralateral PG (D_{mean})	**26.9** [14.3; 50.2]	**21.1** [12.5; 41.2]	**<0.001**
δ index (ideal value = 0)	Ipsilateral PG	**0.41** [-0.05; 0.72]	**0.12** [-0.03; 0.40]	**<0.001**
	Contralateral PG	**0.46** [-0.02; 1.10]	**0.09** [-0.02; 0.41]	**<0.001**
NTCP	Ipsilateral PG	**0.349** [0.060: 0.832]	**0.251** [0.038; 0.668]	**<0.001**
	Contralateral PG	**0.290** [0.099; 0.575]	**0.197** [0.042; 0.504]	**<0.001**

Table 2. Comparison of planned doses, δ index and NTCP (for parotid glands) between standard planning and use of optimized model during planning

A cohort of 30 patients was considered.

			Standard planning Mean [min; max]	**Optimized model method** Mean [min; max]	**p-value**
Dosimetric indexes	**CI (ideal value: 1)**	High-dose PTV	**0.98*** [0.86; 0.99]	**0.98*** [0.86; 0.99]	**0.78**
		Middle-dose PTV	**0.97** [0.88; 1.00]	**0.97** [0.92; 0.99]	**0.04**
		Low-dose PTV	**0.99** [0.96; 1]	**0.99** [0.97; 1]	**0.50**
	HI (ideal value: 0)	High-dose PTV	**0.07** [0.03; 0.15]	**0.09** [0.05; 0.12]	**0.02**
		Middle-dose PTV	**0.17** [0.06; 0.22]	**0.21** [0.14; 0.25]	**<0.001**
		Low-dose PTV	**0.20** [0.10; 0.31)	**0.20** [0.11; 0.29]	**0.52**
Complexity indexes	**MU**		**673.4** [558.0; 845.1]	**744.6** [559.9; 865.0]	**<0.001**
	Area (cm^2) (ideal value: large as possible)		**56.8** [44.0; 78.5]	**50.1** [33.1; 70.1]	**<0.001**
	Irregularity (ideal value: 1)		**13.1** [8.5; 17.4]	**14.0** [9.6; 16.2]	**0.002**
	Modulation ([0;1], ideal value: 0)		**0.8** [0.73; 0.84]	**0.8** [0.76; 0.85]	**<0.001**
Agreement between dose calculation and measurement	**Gamma index passrate (%) (ideal value in our institution: > 85%)**		**94.1** [88.8; 97.6]	**94.6** [84.5; 97.4]	**0.32**

* = normalization point

Table 3. Dosimetric, complexity indexes and gamma index evaluation for standard planning and use of optimized model

Dosimetric and complexity indexes are mean [min; max], for 30 patients. Local gamma analysis (criteria: local, 3%/3 mm, low dose threshold = 30%) was performed between calculation and measurement for standard planning and use of the optimized model (mean [min; max] for 15 patients).

		Standard planning	With optimized model	p-value
CI (ideal value: 1)	High-dose PTV	**0.99** ± *0.01*	**0.98 ±** *0.01*	**0.16**
	Middle-dose PTV	**0.96** ± *0.01*	**0.95** ± *0.02*	**0.02**
	Low-dose PTV	**0.97** ± *0.01*	**0.98** ± *0.01*	**0.20**
HI (ideal value: 0)	High-dose PTV	**0.07** ± *0.01*	**0.09** ± *0.01*	**0.02**
	Middle-dose PTV	**0.17** ± *0.02*	**0.20** ± *0.03*	**0.03**
	Low-dose PTV	**0.14** ± *0.01*	**0.15** ± *0.01*	**0.08**

Table 4. Dosimetric indexes with standard planning and use of optimized model for the inter-operator variability assessment

Dosimetric indexes (conformity and homogeneity) with the standard planning and the use of optimized model are mean ± standard deviation, for 12 different operators.